NASA TECHNICAL NOTE

NASA TN D-7337

COMPARISON OF FINITE-DIFFERENCE
SCHEMES FOR ANALYSIS
OF SHELLS OF REVOLUTION

by Ahmed K. Noor and Wendell B. Stephens

Langley Research Center
Hampton, Va. 23665

1. Report No. NASA TN D-7337	2. Government Accession No.	3. Recipient's Catalog No.
4. Title and Subtitle COMPARISON OF FINITE-DIFFERENCE SCHEMES FOR ANALYSIS OF SHELLS OF REVOLUTION		5. Report Date December 1973
		6. Performing Organization Code
7. Author(s) Ahmed K. Noor and Wendell B. Stephens		8. Performing Organization Report No. L-8898
		10. Work Unit No. 501-22-01-02
9. Performing Organization Name and Address NASA Langley Research Center Hampton, Va. 23665		11. Contract or Grant No.
		13. Type of Report and Period Covered Technical Note
12. Sponsoring Agency Name and Address National Aeronautics and Space Administration Washington, D.C. 20546		14. Sponsoring Agency Code

15. Supplementary Notes

Ahmed K. Noor is Associate Research Professor in Engineering, The George Washington University, Joint Institute for Acoustics and Flight Sciences.

16. Abstract

Several finite-difference schemes are applied to the stress and free-vibration analysis of homogeneous isotropic and layered orthotropic shells of revolution. The study is based on a form of the Sanders-Budiansky first-approximation linear shell theory modified such that the effects of shear deformation and rotary inertia are included. A Fourier approach is used in which all the shell stress resultants and displacements are expanded in a Fourier series in the circumferential direction, and the governing equations reduce to ordinary differential equations in the meridional direction.

While primary attention is given to finite-difference schemes used in conjunction with first-order differential-equation formulation, comparison is made with finite-difference schemes used with other formulations. These finite-difference discretization models are compared with respect to simplicity of application, convergence characteristics, and computational efficiency. Numerical studies are presented for the effects of variations in shell geometry and lamination parameters on the accuracy and convergence of the solutions obtained by the different finite-difference schemes.

On the basis of the present study it is shown that the mixed finite-difference scheme based on the first-order differential-equation formulation and two interlacing grids for the different fundamental unknowns combines a number of advantages over other finite-difference schemes previously reported in the literature.

17. Key Words (Suggested by Author(s)) Finite-difference theory Stress analysis Free vibration Lamination Orthotropism Shells of revolution	18. Distribution Statement Unclassified — Unlimited		
19. Security Classif. (of this report) Unclassified	20. Security Classif. (of this page) Unclassified	21. No. of Pages 43	22. Price* Domestic, $3.00 Foreign, $5.50

COMPARISON OF FINITE-DIFFERENCE SCHEMES

FOR ANALYSIS OF SHELLS OF REVOLUTION

By Ahmed K. Noor* and Wendell B. Stephens
Langley Research Center

SUMMARY

Several finite-difference schemes are applied to the stress and free-vibration analysis of homogeneous isotropic and layered orthotropic shells of revolution. The study is based on a form of the Sanders-Budiansky first-approximation linear shell theory modified such that the effects of shear deformation and rotary inertia are included. A Fourier approach is used in which all the shell stress resultants and displacements are expanded in a Fourier series in the circumferential direction, and the governing equations reduce to ordinary differential equations in the meridional direction.

While primary attention is given to finite-difference schemes used in conjunction with first-order differential-equation formulation, comparison is made with finite-difference schemes used with other formulations. These finite-difference discretization models are compared with respect to simplicity of application, convergence characteristics, and computational efficiency. Numerical studies are presented for the effects of variations in shell geometry and lamination parameters on the accuracy and convergence of the solutions obtained by the different finite-difference schemes.

On the basis of the present study it is shown that the mixed finite-difference scheme based on the first-order differential-equation formulation and two interlacing grids for the different fundamental unknowns combines a number of advantages over other finite-difference schemes previously reported in the literature.

INTRODUCTION

In the past decade a substantial capability has been developed for the numerical analysis of rotationally symmetric shells. The most widely used numerical analysis procedures for this class of shells are those based on numerical integration, finite elements, and finite differences. A number of publications exist which review and assess the relative merits of these three numerical techniques (see, for example, refs. 1, 2, and 3).

---

*Associate Research Professor in Engineering, The George Washington University, Joint Institute for Acoustics and Flight Sciences.

The large majority of existing finite-difference programs for rotationally symmetric shells are based on either the displacement formulation (with the fundamental unknowns being displacement parameters) (ref. 4), or the Budiansky-Radkowski second-order differential-equation formulation (refs. 1, 5, and 6). While the advantages of using a first-order differential-equation formulation have been widely recognized in numerical integration techniques and in matrix progression method (refs. 7 to 11), only limited use of this formulation has been made in the case of finite differences (refs. 12 and 13).

The objective of this paper is to assess the relative merits of several finite-difference schemes used for the linear elastic stress and free-vibration analysis of rotationally symmetric shells. Primary attention is given to mixed finite-difference schemes used in conjunction with the first-order ordinary-differential-equation formulation. However, some consideration is given to finite-difference schemes used with the displacement formulation and with the Budiansky-Radkowski second-order differential equations.

The term "mixed" refers to the fact that both stress resultants and displacements are chosen as primary variables. The analytical formulation is based on the Sanders-Budiansky linear shell theory. The first-order ordinary-differential-equation formulation of that theory is modified such that the effects of shear deformation and rotary inertia are included.

SYMBOLS

A_{ij} $\quad$ $(i,j = 1,2, \ldots,5)$

B_{ij},G_{ij} $\quad$ $(i,j=1,2,3)$

$\left.\right\}$ dimensionless elastic compliance coefficients of the shell

$b_1,b_2, \ldots,b_7,b_c$ $\qquad$ dimensionless elastic coefficients of the shell

C_{ij},F_{ij},D_{ij} $\quad$ $(i,j=1,2,3)$ $\qquad$ dimensionless elastic stiffnesses of the shell

$\tilde{C}_0$ $\qquad$ reference extensional rigidity of the shell

$c_{ij}^{(k)}$ $\quad$ $(i,j=1,2, \ldots,5)$ $\qquad$ elastic stiffness of the kth layer of the shell

$d = \dfrac{d}{d\xi}$

E	elastic modulus for isotropic materials
E_f	error index (see eq. (19))
E_L, E_T	elastic moduli in the direction of the fibers and normal to it, respectively
G_{LT}, G_{TT}	shear moduli in the plane of the fibers and normal to it, respectively
h	local thickness of the shell (see fig. 1)
h_k, h_{k-1}	distance from the reference (middle) surface to the top and bottom surfaces of the kth layer, respectively
$i = \sqrt{-1}$	
L	reference length of the shell
ℓ	finite-difference interval in the meridional direction
$M_\xi, M_\theta, M_{\xi\theta}, M_{\theta\xi}$	moment stress resultants (see fig. 2)
m	Fourier harmonic in the circumferential direction
$N_\xi, N_\theta, N_{\xi\theta}, N_{\theta\xi}$	direct stress resultants (see fig. 2)
$\tilde{N}_{\xi\theta}$	modified (boundary) stress resultant
$\overline{N}_{\xi\theta}, \overline{M}_{\xi\theta}$	symmetric stress resultants
NL	number of layers of laminated shells
n	number of finite-difference intervals in the meridional direction
$P_{1,m}, P_{2,m}$	vectors of external forces
p_o	amplitude of load harmonic
p_r, p_θ, p_ξ	intensity of external loading in the coordinate directions (see fig. 2)

Q_ξ, Q_θ	transverse shear stress resultants (see fig. 2)
R	radius of toroidal cross section
R_1, R_2	principal radii of curvature in the meridional and circumferential directions, respectively
r	normal distance from the shell axis to the reference surface (see fig. 1)
t	time
U_ξ, U_θ, W	displacement components of the reference surface in the coordinate directions (see fig. 2)
x_1, x_2, x_3	curvilinear coordinate system (see fig. 1)
λ, λ_1	dimensionless frequencies
ν	Poisson's ratio for isotropic materials
ν_{LT}	Poisson's ratio measuring strain in T-direction due to uniaxial normal stress in the L-direction
ξ, θ	dimensionless meridional and circumferential coordinates, respectively (see fig. 1)
$\rho_s^{(k)}$	density of the kth layer of laminated shells

$$\left. \begin{array}{l} \rho = \dfrac{r}{L} \\[2ex] \omega_\xi = \dfrac{L}{R_1} \\[2ex] \omega_\theta = \dfrac{L}{R_2} \\[2ex] \gamma = \dfrac{d\rho/d\xi}{\rho} \end{array} \right\} \quad \text{nondimensional geometric parameters}$$

4

ϕ_ξ, ϕ_θ	rotation components (see fig. 2)
$\{\psi_m\}$ and $\{H_m\}$	vectors of fundamental unknowns defined by equations (14) and (15)
ω	circular frequency of vibration of the shell
$\lfloor \ \rceil$	row matrix
$\{\ \}$	column matrix
$[\ ]$	rectangular or square matrix

Subscripts:

i	generic finite-difference station
L,T	denote the direction of fibers and the transverse direction
m	denotes the mth Fourier harmonic

Finite-difference models:

DW	displacement formulation, whole-station scheme
SW	second-order formulation, whole-station scheme
MW	mixed formulation, whole-station scheme
MHS 1, MHS 2	mixed formulation, half-station scheme, single grid
MHI	mixed formulation, half-station scheme, interlacing grid

MATHEMATICAL FORMULATION

Shell Geometry

Figure 1 shows the geometric characteristics of a rotationally symmetric shell as follows: h is the local thickness of the shell; r is the normal distance from the shell axis to the reference surface; R_1 and R_2 are the principal radii of curvature in the meridional and circumferential directions, respectively. The expressions for R_1 and R_2 are given in reference 5.

To cast the problem in nondimensional form, the two dimensionless coordinates ξ and θ are used, where

$$\xi = \frac{x_1}{L} \tag{1}$$

$$\theta = \frac{x_2}{r} \tag{2}$$

in which x_1 and x_2 are the meridional and circumferential coordinates, respectively, and L is a reference length.

Also, as in reference 5, the following dimensionless geometric parameters are introduced:

$$\rho = \frac{r}{L} \tag{3}$$

$$\omega_\xi = \frac{L}{R_1} \tag{4}$$

$$\omega_\theta = \frac{L}{R_2} \tag{5}$$

and

$$\gamma = \frac{d\rho/d\xi}{\rho} \tag{6}$$

Reduction to a One-Dimensional Problem

The analytical formulation is based on a form of the Sanders-Budiansky linear theory modified such that the effects of shear deformation and rotary inertia are included.

If the shell stress resultants and displacements as well as the external loads are expanded in a Fourier series in the circumferential direction, then

$$\left\lfloor U_\xi \ W \ \phi_\xi \ N_\xi \ M_\xi \ Q_\xi \right\rfloor = \sum_{m=0}^{\infty} \left\lfloor U_{\xi,m} \ W_m \ \phi_{\xi,m} \ N_{\xi,m} \ M_{\xi,m} \ Q_{\xi,m} \right\rfloor \cos m\theta \tag{7}$$

$$\left[U_\theta \quad \phi_\theta \quad \tilde{N}_{\xi\theta} \quad \overline{M}_{\xi\theta} \quad Q_\theta \right] = \sum_{m=0}^{\infty} \left[U_{\theta,m} \quad \phi_{\theta,m} \quad N_{\xi\theta,m} \quad M_{\xi\theta,m} \quad Q_{\theta,m} \right] \sin m\theta \qquad (8)$$

$$\left[p_\xi \quad p_r \right] = \sum_{m=0}^{\infty} \left[p_{\xi,m} \quad p_{r,m} \right] \cos m\theta \qquad (9)$$

and

$$p_\theta = \sum_{m=0}^{\infty} p_{\theta,m} \sin m\theta \qquad (10)$$

where

$$\tilde{N}_{\xi\theta} = \overline{N}_{\xi\theta} + \left\{ \frac{\omega_\theta - \omega_\xi}{2L} \right\} \overline{M}_{\xi\theta} \qquad (11)$$

in which $\overline{N}_{\xi\theta}$ and $\overline{M}_{\xi\theta}$ are the modified (symmetric) stress resultants defined in reference 5.

For free-vibration analysis, the right-hand sides of equations (7) and (8) must be multiplied by $e^{i\omega t}$ where ω is the circular frequency of vibration of the shell.

Governing Differential Equations

The stress and free-vibration problems for shells of revolution can be formulated in a number of different ways. For example, such problems can be formulated in terms of (1) the three displacement components of the reference surface, (2) coupled second-order ordinary differential equations in the generalized displacements and meridional moment stress resultant, or (3) first-order ordinary differential equations in the shell stress resultants and displacements. In the absence of shear deformation, the governing equations of the displacement formulation for cylindrical shells are given in reference 14, and the governing equations of the second-order formulation for general shells of revolution are presented in references 1 and 5. These equations are not reproduced here. On the other hand, the first-order equation formulation which has been extensively studied herein is outlined below. Discussion is focused on the choice of the fundamental unknowns and the form of governing differential equations in such a way as to enhance the computational efficiency of the finite-difference discretization.

The fundamental unknowns of the first-order differential-equation formulation used herein are chosen to be the shell quantities that appear in the statement of the boundary (or interface) conditions along a parallel circle. These include: the five generalized

displacements U_ξ, U_θ, W, ϕ_ξ, and ϕ_θ; and the five stress resultants N_ξ, $\tilde{N}_{\xi\theta}$, Q_ξ, M_ξ, and $\overline{M}_{\xi\theta}$ (see fig. 2).

By properly ordering the fundamental unknowns, the governing differential equations for the mth Fourier harmonic can be arranged to yield a symmetric coefficient matrix of the fundamental unknowns as follows:

$$\begin{bmatrix} S^a & \vdots & S \\ \cdots & \vdots & \cdots \\ S^T & \vdots & S^b \end{bmatrix} \begin{Bmatrix} H_m \\ \cdots \\ \psi_m \end{Bmatrix} + \begin{bmatrix} 0 & \vdots & I_1 \\ \cdots & \vdots & \cdots \\ -I_1 & \vdots & 0 \end{bmatrix} \begin{Bmatrix} dH_m \\ \cdots \\ d\psi_m \end{Bmatrix} + \omega^2 \begin{bmatrix} m^a & \vdots & 0 \\ \cdots & \vdots & \cdots \\ 0 & \vdots & m^b \end{bmatrix} \begin{Bmatrix} H_m \\ \cdots \\ \psi_m \end{Bmatrix} + \begin{Bmatrix} P_{1,m} \\ P_{2,m} \end{Bmatrix} = 0 \qquad (12)$$

where

$$d \equiv \frac{d}{d\xi} \qquad (13)$$

$$\{H_m\}^T \doteq \begin{bmatrix} \dfrac{\rho N_{\xi,m}}{\tilde{C}_o} ; & \dfrac{\rho M_{\xi,m}}{L\tilde{C}_o} ; & \dfrac{U_{\theta,m}}{L} ; & \dfrac{W_m}{L} ; & \phi_{\theta,m} \end{bmatrix} \qquad (14)$$

$$\{\psi_m\}^T = \begin{bmatrix} \dfrac{U_{\xi,m}}{L} ; & \phi_{\xi,m} ; & \dfrac{\rho N_{\xi\theta,m}}{\tilde{C}_o} ; & \dfrac{\rho Q_{\xi,m}}{\tilde{C}_o} ; & \dfrac{\rho M_{\xi\theta,m}}{L\tilde{C}_o} \end{bmatrix} \qquad (15)$$

The term $\tilde{C}_o$ is a reference extensional rigidity of the shell. The shell stiffnesses and compliances are given in appendix A. The $[S^a]$, $[S^b]$, and $[S]$ are 5×5 matrices, the first two matrices are symmetric; superscript T denotes transposition; the matrix $[I_1]$ is a diagonal matrix; $[m^a]$ and $[m^b]$ are symmetric mass matrices; and $\{P_{1,m}\}$ and $\{P_{2,m}\}$ are vectors of external forces. The formulas for the coefficients of the aforementioned matrices are given in appendix B. For stress-analysis problems $\omega = 0$ and for free-vibration problems $\{P_{1,m}\} = \{P_{2,m}\} = 0$.

The choice of the fundamental unknowns shown in equations (14) and (15) is similar to that suggested by Goldberg (ref. 7); however, the present formulation utilizes the geometric parameter $\rho(\xi)$ in defining the unknowns for stress resultants. This particular choice allows casting the governing equations in a symmetric form and minimizes the number of nonzero terms in the matrix $[S]$.

FINITE-DIFFERENCE DISCRETIZATION

The finite-difference models used with the displacement and second-order differential-equation formulation were based on the whole-station approximation. These two models will be referred to subsequently as DW (displacement, whole-station) and SW (second-order, whole-station) schemes. The latter model, SW, was first suggested by Budiansky and Radkowski (ref. 5) and developed into an operational program "SALORS" in reference 15. Since the DW and SW schemes have been discussed in references 14 and 15, the discussion is confined here to the discretization of the first-order differential equations. To this end, it is convenient to express equations (12) as follows:

$$\left[S^a\right]\left\{H_m\right\} + \left[S\right]\left\{\psi_m\right\} + \left[I_1\right]\left\{d\psi_m\right\} = -\omega^2\left[m^a\right]\left\{H_m\right\} - \left\{P_{1,m}\right\} \tag{16a}$$

and

$$\left[S^b\right]\left\{\psi_m\right\} + \left[S\right]^T\left\{H_m\right\} - \left[I_1\right]\left\{dH_m\right\} = -\omega^2\left[m^b\right]\left\{\psi_m\right\} - \left\{P_{2,m}\right\} \tag{16b}$$

Four finite-difference models have been used for the discretization of equations (16). These models differ by the difference-quotient expressions used for approximating the first derivatives and by the location of the points at which the difference equations are applied. The four models can be identified as mixed whole station (MW), mixed half-station, single grid (MHS 1 and MHS 2), and mixed half-station, interlacing grid scheme (MHI). The two schemes MHS 1 and MHS 2 differ one from the other in the difference-quotient expressions used for approximating the first derivatives. For shells with constant elastic and geometric characteristics, the discrete models obtained by these two schemes are identical.

The characteristics of the four finite-difference models MW, MHS 1, MHS 2, and MHI along with those of the two models DW and SW are summarized in table 1. While three of the four schemes used with the first-order equation formulation, schemes MW, MHS 1, and MHS 2, have been reported previously in the literature, the fourth scheme (MHI) which was developed by the authors represents the prime thrust of the present work and is described in detail below. It should be noted, however, that other interlacing grids have been suggested and used previously by others (e.g., refs. 4 and 16).

The basic idea of the mixed half-station interlacing-grid scheme (MHI) used in the present study is to define the first derivatives of each of the fundamental unknowns at points lying midway between the points of definition of the same unknowns. This can be accomplished by using two sets of interlacing grids for the two groups of fundamental unknowns $\left\{H_m\right\}$ and $\left\{\psi_m\right\}$. The quantities $\left\{\psi_m\right\}$ and $\left\{dH_m\right\}$ in equations (16) are

defined at points lying midway between the points of definition of $\{H_m\}$ and $\{d\psi_m\}$. For convenience both $\{H_m\}$ and $\{\psi_m\}$ are defined at the boundaries and interfaces.

The finite-difference equations which simulate the governing equations (eqs. (16)) are obtained by replacing the first derivatives in these equations by an appropriate difference-quotient expression, depending on the order of approximation desired (see ref. 17).

Also, due to the coupling between $\{\psi_m\}$ and $\{d\psi_m\}$ in equations (16a) and between $\{H_m\}$ and $\{dH_m\}$ in equations (16b) (i.e., due to the presence of the matrix $[S]$), the values of $\{\psi_m\}$ in the first equation and $\{H_m\}$ in the second equation have to be obtained through interpolation between their values at their respective control points. As will be shown subsequently, the accuracy of solutions is less sensitive to this interpolation than to the averaging of the difference-quotient expressions, which is used in conventional schemes (with all the fundamental unknowns and their derivatives defined at the same set of points).

In order to maintain the number of unknowns equal to the number of equations, only the five equations (16a) are applied at the boundary, the other five equations are replaced by the five boundary conditions. The accuracy of the modified scheme presented herein, however, was found to be insensitive to the particular choice of the five equations to be applied at the boundary. A summary of the equations applied at the different nodal points is given in figure 3. Central differences are used at interior points and backward (or forward) unsymmetric differences are used at points lying on or near the boundaries (or interfaces). The number of such specialized unsymmetric difference formulas is dependent on the order of the interior discretization error used in the finite-difference scheme (see ref. 17).

As an illustration, the difference equations are shown for the MHI scheme. These difference equations of order $O(\ell^2)$, where ℓ is the finite-difference interval, at generic interior points i and $i+1$, are given by

$$[S^a]_i \{H_m\}_i + \left[\frac{-1}{\ell} [I_1] + \frac{1}{2} [S]_i\right] \{\psi_m\}_{i-1} + \left[\frac{1}{\ell} [I_1] + \frac{1}{2} [S]_i\right] \{\psi_m\}_{i+1}$$

$$= -\alpha^2 [m^a]_i \{H_m\}_i - \{P_{1,m}\}_i \qquad (17a)$$

$$[S^b]_{i+1} \{\psi_m\}_{i+1} + \left[\frac{1}{\ell} [I_1] + \frac{1}{2} [S]_{i+1}^T\right] \{H_m\}_i + \left[\frac{-1}{\ell} [I_1] + \frac{1}{2} [S]_{i+1}^T\right] \{H_m\}_{i+2}$$

$$= -\alpha^2 [m^b]_{i+1} \{\psi_m\}_{i+1} - \{P_{2,m}\}_{i+1} \qquad (17b)$$

10

The resulting finite-difference field equations can be represented in the following compact form:

$$[K_m]\{Z_m\} = -\omega^2[\tilde{m}]\{Z_m\} - \{\tilde{P}_m\} \tag{18}$$

where $[K_m]$ and $[\tilde{m}]$ contain the generalized stiffness and mass distribution, $\{Z_m\}$ is the vector of unknowns composed of the subvectors $\{H_m\}_i$ and $\{\psi_m\}_{i\pm1}$ at the various finite-difference stations and $\{\tilde{P}_m\}$ is the vector of external forces and thermal effects. Equations (18) are banded and their bandwidth depends on the orders of the interior and boundary approximations. The use of interlacing grids results in reducing both the interior discretization error and the bandwidth of the resulting finite-difference equations and, therefore, the computational efficiency of the scheme is improved. That this is indeed so can be seen from figure 4, where a schematic representation is given of the finite-difference equations corresponding to the four schemes MW, MHS1, MHS2, and MHI.

The four finite-difference schemes MW, MHS 1, MHS 2, and MHI have a number of advantages also shared with other numerical approximation techniques based on the first-order equation formulation. These include the simplicity of the form of the governing differential equations, the absence of the derivatives of the elastic characteristics of the shell in these equations, and the simplicity of numerical discretization and of handling the boundary and interface conditions. As a result of the cited advantages, the effort required in the computer implementation of these difference schemes (coding, debugging, and verification) has been found to be significantly reduced.

EIGENVALUE EXTRACTION TECHNIQUE

For free-vibration problems, a variant of the inverse-power method with shifts similar to that presented in reference 1 is used for the determination of the natural frequencies and mode shapes. In the present study, advantage was taken of the banded form of the matrix $[K_m]$ and a direct, Gaussian elimination procedure was used for each iteration to evaluate the new trial vector $\{Z_m\}$.

NUMERICAL STUDIES

In an attempt to assess the relative merits of the different finite-difference schemes, a large number of stress and free-vibration problems of homogeneous isotropic and layered orthotropic shells of revolution were solved using the aforementioned six finite-difference schemes.

The various finite-difference models are compared with respect to simplicity of application, convergence characteristics, and computational efficiency. The results of four typical problem sets representing different shell geometries and wall construction are discussed with respect to convergence characteristics herein. These problems are:

a. Free vibrations of isotropic cylindrical shell
b. Asymmetric stresses in isotropic toroidal shell subjected to a uniform normal pressure
c. Asymmetric free vibrations of layered orthotropic toroidal shell
d. Free vibrations of layered orthotropic spherical shells

The four difference models based on the first-order equation formulation (MW, MHS 1, MHS 2, and MHI schemes) were applied to all four problems, and the second-order equation model (SW scheme) was applied to the first two problems. Comparison was made with the results obtained using the displacement model (DW scheme) for the first problem (ref. 14).

In the first two problems in order to provide a meaningful comparison with finite-difference schemes SW and DW, the tracing constants k_r and k_α (where $\alpha = 1,2$) in the appropriate equations in appendix B, were set equal to 0 and 10^4, respectively. This resulted in dropping the rotary inertia terms and suppressing the shear deformation in these problems.

Free Vibrations of Cylindrical Shells

The first problem considered was that of asymmetric free vibrations of isotropic cylindrical shells with clamped edges. The characteristics of the shells considered are shown in figure 5. This problem was taken from reference 14 where it was concluded that the accuracy of the finite-difference method, based on a differential-equation formulation in terms of the three midsurface displacements, deteriorates rapidly as the length ratio L/R increases or the thickness ratio h/R decreases. Therefore, in order to assess the accuracy and rate of convergence for the six finite-difference schemes, the long thin shell shown in figure 5 was selected. For this problem it was found that both the shear deformation and rotary inertia were negligible and, therefore, the use of schemes DW and SW is justified.

The nondimensional minimum frequencies obtained by the different finite-difference schemes are summarized in table 2 and the corresponding mode shapes and modal stresses obtained by schemes MHS 1, MHS 2, and MHI with 20 finite-difference intervals are shown in figure 6.

As is seen from this figure the three schemes MHS 1, MHS 2, and MHI accurately predict the mode shape and the modal stress-resultant N_ξ, but for the modal moment M_ξ, scheme MHI misses the spike at the boundaries and schemes MHS 1 and MHS 2 give an oscillatory type of variation.

The results presented in table 2 show that the frequencies obtained by the mixed half-station interlacing grid finite-difference scheme (MHI) are more accurate than the corresponding frequencies obtained by other schemes (for the same number of finite-difference intervals). The error in the frequency obtained by using MHI scheme with 10 finite-difference intervals is only 1.5 percent. On the other hand, the frequencies obtained by DW and SW schemes (based on the displacement and the four second-order equations) are considerably less accurate than those obtained by all other schemes based on the use of first-order differential-equation formulation. Also, the frequencies obtained by DW and SW schemes are identical to four significant digits. This is because the discretized equations in the SW scheme for cylindrical shells can be reduced to sets of equations identical to those obtained by direct discretization of the three differential equations of the displacement formulation, DW scheme (see ref. 17). Similar reasoning can be used to explain the fact that the frequencies obtained by MHS 1 and MHS 2 schemes are identical and those obtained by the MHI scheme are identical to the ones obtained by the MW scheme using twice as many finite-difference intervals (compare the corresponding entries in table 2).

Stress Analysis of a Closed Toroidal Shell

As a second example consider the asymmetric stress analysis of an isotropic closed toroidal shell subjected to a normal pressure which is uniform in the meridional direction. The characteristics of the shell and loading are shown in figure 7.

Solutions have been obtained using the finite-difference schemes SW, MW, MHS 1, MHS 2, and MHI for the asymmetric stress analysis for an internal pressure loading which is uniform in the meridional direction. Only the second Fourier harmonic in the circumferential direction is considered ($m = 2$). For this shell and loading, the shear deformation was found to be negligible and therefore the use of scheme SW is justified. Due to symmetry of the shell and loading, only half the meridian was considered and the symmetric boundary conditions at the ends are $\{\psi_m\} = 0$.

As a quantitative measure of the relative accuracy of the stress resultants and displacements obtained by the different finite-difference schemes, the following error index E_f (a function of f) has been introduced:

$$E_f = \frac{1}{n+1} \sqrt{\sum_{i=1}^{n+1} \left(\frac{f_i - \tilde{f}_i}{|f_{max}|}\right)^2} \tag{19}$$

where

f stands for any of the stress resultants or generalized displacements

f_i and $\tilde{f}_i$ are the exact and approximate values, respectively, of the function at the ith finite-difference station. The exact value is taken to be the converged solution, and the approximate value refers to the value obtained by each of the finite-difference schemes.

$|f_{max}|$ is the maximum absolute value of the exact (or converged) function in the interval of interest (half the meridian of the shell in this case).

n+1 is the total number of finite-difference stations used in the approximate solution.

In order to simplify comparison with other schemes, the values of the unknowns $\{\psi_m\}$ in scheme MHI were computed at the same nodal points as the unknowns $\{H_m\}$. This was done after obtaining the modified solution. As an example, at the node point i

$$\{\psi_m\}_i = \frac{1}{2}\left\{\{\psi_m\}_{i-1} + \{\psi_m\}_{i+1}\right\}$$

where $\{\psi_m\}_{i-1}$ and $\{\psi_m\}_{i+1}$ are the values of $\{\psi_m\}$ at points i∓1 obtained from the modified solution.

While the error index E_f (eq. (19)) is similar to the root-mean-square error, it has the added advantage that it gives less weight to the smaller values of the function, which are usually of less practical interest. The smaller the error index E_f, the more accurate the approximate solution (obtained by the difference scheme) is.

The values of the error index E_f for each of the stress resultants and generalized displacements obtained by the different finite-difference schemes using 10, 20, 30, and 40 intervals in half the shell meridian are summarized in table 3. Also, figure 8 shows plots for the stress resultants and displacements obtained by schemes SW, MW, and MHI. Also shown are the essentially exact results (converged solution) for this problem. Solutions obtained by schemes MHS 1 and MHS 2 are not shown in order to avoid complicating the figure. To provide a reasonable comparison among the three finite-difference solutions shown in figure 8, the total number of algebraic equations for each method was made

14

comparable. This was achieved by using 10 finite-difference intervals in half the shell meridian in schemes MW and MHI and 20 intervals for scheme SW. Note that if the shear deformation is neglected, the governing differential equations used in schemes MW and MHI reduce to eight and the total number of algebraic equations for each method will almost be identical. Figure 8 and table 3 clearly show the high accuracy of the predictions of the proposed scheme (MHI) and that this accuracy occurs for both displacement and stress quantities in this case.

Moreover, it was found that the accuracy of the solutions obtained by scheme MW was very sensitive to the particular choice of the five equations applied at the boundary. The best accuracy was obtained when the boundary conditions were applied in a manner similar to that used in finite-element method, wherein the 10 equations (eqs. (12)) are applied at the boundary, then the boundary conditions replace the equations with the specified boundary quantities (in this case displacement, rotation components, and stress resultants) appearing along the diagonal. The results shown in table 3 for scheme MW were obtained for the aforementioned choice. On the other hand, the accuracy of the solutions obtained by scheme MHI was found to be insensitive to the choice of the 5 equations to be applied at the boundary.

Asymmetric Free Vibrations of Laminated Orthotropic Toroidal Shell

In order to study the effect of material orthotropy of the shell on the accuracy and rate of convergence of the different finite-difference schemes, the free-vibration problem of an eight-layered, graphite-epoxy composite shell was studied. The shell had the same dimensions and total thickness as that of the isotropic shell considered previously (see fig. 7). Both shear deformation and rotary inertia were accounted for and consequently scheme SW was not used.

An indication of the accuracy and rate of convergence of the minimum frequency obtained by schemes MW, MHS 1, MHS 2, and MHI is shown in figure 9. The results obtained by schemes MHS 1 and MHS 2 were almost identical. As shown in figure 9 the frequencies obtained by all schemes converged to the same value, but those obtained by scheme MHI had a faster rate of convergence.

Free Vibrations of Layered Composite Spherical Shell Segment

As a final example consider the free vibrations of an eight layered, graphite-epoxy spherical-shell segment with clamped edges. The fibers of the different layers alternate between the circumferential and meridional directions, with the fibers of the top layer running in the meridional direction. Shells with different rise ratios, ranging from

shallow to deep shells, have been studied. The characteristics of these shells are shown in figure 10. For all these shells solutions were obtained using the first order difference models (schemes MW, MHS 1, MHS 2, and MHI).

The solutions obtained using the different schemes are summarized in table 4. As can be seen from this table scheme MHI is superior to all other schemes. The accuracy of the solutions obtained by this scheme does not deteriorate as the shell becomes shallower.

CONCLUDING REMARKS

A comparison is made between a number of finite-difference schemes for analysis of shells of revolution. Primary attention is given to finite-difference schemes based on the use of first-order ordinary differential-equation formulation; however, some consideration is given to both the displacement and the second-order differential-equation models. The various finite-difference discretization models are compared with respect to simplicity of application, convergence characteristics, and computational efficiency.

On the basis of the present study it is shown that the mixed finite-difference schemes have a number of major advantages in common with other numerical approximation techniques based on the first-order differential-equation formulation. These include the simplicity of the form of the governing differential equations, the absence of the derivatives of the elastic characteristics of the shell in these equations, and the simplicity of numerical discretization and of handling boundary and interface conditions. A proper selection of the fundamental unknowns and a proper ordering of the governing equations can lead to further simplifications which produces a symmetric coefficient matrix in the governing equations. Of all the finite-difference schemes used with the first-order equation formulation, the scheme presented herein, which is based on the use of the two interlacing grids for the different fundamental unknowns, leads to the minimum bandwidth of the finite-difference field equations and the maximum accuracy of the solution and, therefore, is computationally most efficient.

Langley Research Center,
National Aeronautics and Space Administration,
Hampton, Va., September 19, 1973.

16

APPENDIX A

ELASTIC COEFFICIENTS OF LAMINATED SHELLS

Elastic Stiffnesses of the Layers

The stiffness coefficients of the kth orthotropic layer of the shell are given by:

$$\left[c_{ij}^{(k)}\right] = \begin{bmatrix} \dfrac{E_L^{(k)}}{\bar{\lambda}^{(k)}} & \nu_{LT}^{(k)}\dfrac{E_L^{(k)}}{\bar{\lambda}^{(k)}} & 0 \\ & \dfrac{E_T^{(k)}}{\bar{\lambda}^{(k)}} & 0 \\ \text{Symmetric} & & G_{LT}^{(k)} \end{bmatrix} \qquad \begin{pmatrix} i = 1,2,3 \\ j = 1,2,3 \end{pmatrix} \quad (A1)$$

and

$$\left[c_{ij}^{(k)}\right] = \begin{bmatrix} G_{TT}^{(k)} & 0 \\ 0 & G_{LT}^{(k)} \end{bmatrix} \qquad \begin{pmatrix} i = 4,5 \\ j = 4,5 \end{pmatrix} \quad (A2)$$

where subscripts L and T denote the direction of fibers and the transverse direction, ν_{LT} is the Poisson's ratio measuring the strain in the T-direction due to a uniaxial normal stress in the L-direction,

$$\left. \begin{aligned} \nu_{LT}E_L &= \nu_{TL}E_T \\[2ex] \bar{\lambda} &= 1 - \nu_{LT}\nu_{TL} \end{aligned} \right\} \qquad (A3)$$

and superscript k refers to the kth layer.

Elastic Coefficients of the Shell

The dimensionless elastic stiffnesses of the shell are given by:

$$\begin{bmatrix} C_{ij} & F_{ij} & D_{ij} \end{bmatrix} = \frac{1}{\tilde{C}_o} \sum_{k=1}^{NL} \int_{h_{k-1}}^{h_k} c_{ij}^{(k)} \begin{bmatrix} 1 & \dfrac{x_3}{L} & \dfrac{x_3^2}{L^2} \end{bmatrix} dx_3 \qquad \begin{pmatrix} i = 1,2,3 \\ j = 1,2,3 \end{pmatrix} \quad (A4)$$

and

$$C_{ij} = \frac{1}{\tilde{C}_o} \sum_{k=1}^{NL} \int_{h_{k-1}}^{h_k} c_{ij}^{(k)} \, dx_3 \qquad \begin{pmatrix} i = 4,5 \\ j = 4,5 \end{pmatrix} \quad (A5)$$

where

NL = total number of layers of the shell

h_k and h_{k-1} are the distances from the reference surface to the top and bottom surfaces of the kth layer, respectively

$\tilde{C}_o$ is a reference extensional rigidity of the shell

The dimensionless elastic compliances of the shell A_{ij}, B_{ij}, G_{ij} (i,j = 1,2,3) and A_{ij} (i,j = 4,5) are obtained by inversion of the matrix of the elastic stiffnesses as follows:

$$\begin{bmatrix} A & \vdots & B \\ \cdots & + & \cdots \\ B & \vdots & G \end{bmatrix} = \begin{bmatrix} C & \vdots & F \\ \cdots & + & \cdots \\ F & \vdots & D \end{bmatrix}^{-1} \qquad \begin{bmatrix} A_{ij} \end{bmatrix} = \begin{bmatrix} C_{ij} \end{bmatrix}^{-1} \qquad \begin{pmatrix} i = 4,5 \\ j = 4,5 \end{pmatrix}$$

The elastic stiffnesses and compliances of the shell are functions of the meridional coordinate ξ.

APPENDIX B

FORMULAS FOR COEFFICIENTS IN GOVERNING
DIFFERENTIAL EQUATIONS

The independent nonzero terms of the submatrices $\left[S^a\right]$, $\left[S^b\right]$, and $[S]$ in equations (17) are given by:

$$S^a_{11} = \frac{b_1}{\rho}$$

$$S^a_{12} = \frac{b_2}{\rho}$$

$$S^a_{13} = \frac{mb_c b_3}{\rho}$$

$$S^a_{14} = \omega_\theta b_c b_3 - \omega_\xi$$

$$S^a_{15} = \frac{mb_c b_4}{\rho}$$

$$S^a_{22} = \frac{b_5}{\rho}$$

$$S^a_{23} = \frac{mb_c b_6}{\rho}$$

$$S^a_{24} = \omega_\theta b_c b_6$$

$$S^a_{25} = \frac{mb_c b_7}{\rho}$$

$$S^a_{33} = -\frac{m^2 b_c G_{22}}{\rho} - \frac{\rho \omega_\theta^2 k_2}{A_{55}}$$

$$S^a_{34} = -m\omega_\theta \left(b_c G_{22} + \frac{k_2}{A_{55}} \right)$$

$$S^a_{35} = \frac{m^2 b_c B_{22}}{\rho} + \frac{\rho \omega_\theta k_2}{A_{55}}$$

$$S_{44}^a = -b_c \omega_\theta^2 G_{22} \rho - \frac{m^2 k_2}{\rho A_{55}}$$

$$S_{45}^a = m \left(b_c B_{22} \omega_\theta + \frac{k_2}{A_{55}} \right)$$

$$S_{55}^a = - \frac{m^2 b_c A_{22}}{\rho} - \frac{\rho k_2}{A_{55}}$$

$$S_{11}^b = -b_c \rho \gamma^2 G_{22}$$

$$S_{12}^b = \rho b_c \gamma^2 B_{22}$$

$$S_{13}^b = \frac{m}{\rho}$$

$$S_{14}^b = \omega_\xi$$

$$S_{15}^b = \frac{-m \left(\omega_\theta - \omega_\xi \right)}{\rho}$$

$$S_{22}^b = -b_c \rho \gamma^2 A_{22}$$

$$S_{24}^b = -1$$

$$S_{25}^b = \frac{m}{\rho}$$

$$S_{33}^b = \frac{A_{33}}{\rho}$$

$$S_{35}^b = \frac{-\frac{1}{2} \left(\omega_\theta - \omega_\xi \right) A_{33} + B_{33}}{\rho}$$

$$S_{44}^b = \frac{A_{44}}{\rho k_1}$$

$$S_{55}^b = \frac{\frac{1}{4}\left(\omega_\theta - \omega_\xi\right)^2 A_{33} - \left(\omega_\theta - \omega_\xi\right) B_{33} + G_{33}}{\rho}$$

$$S_{11} = b_c \gamma b_3$$

$$S_{12} = b_c \gamma b_4$$

$$S_{21} = b_c \gamma b_6$$

$$S_{22} = b_c \gamma b_7$$

$$S_{31} = -m b_c \gamma G_{22}$$

$$S_{32} = m b_c \gamma B_{22}$$

$$S_{33} = \gamma$$

$$S_{35} = -\gamma \left(\omega_\theta - \omega_\xi\right)$$

$$S_{41} = -b_c \rho \gamma G_{22} \omega_\theta$$

$$S_{42} = b_c \rho \gamma B_{22} \omega_\theta$$

$$S_{51} = m b_c \gamma B_{22}$$

$$S_{52} = -m b_c \gamma A_{22}$$

$$S_{55} = \gamma$$

where b_1 to b_7 are dimensionless coefficients given by:

$$b_1 = A_{11} + b_c \left\{ -A_{12} \left(A_{12}G_{22} - B_{12}B_{22} \right) + B_{12} \left(A_{12}B_{22} - A_{22}B_{12} \right) \right\}$$

$$b_2 = B_{11} - b_c \left\{ A_{12} \left(B_{12}G_{22} - B_{22}G_{12} \right) + B_{12} \left(A_{22}G_{12} - B_{12}B_{22} \right) \right\}$$

$$b_3 = A_{12}G_{22} - B_{12}B_{22}$$

$$b_4 = -A_{12}B_{22} + A_{22}B_{12}$$

$$b_5 = G_{11} - b_c \left\{ B_{12} \left(B_{12}G_{22} - B_{22}G_{12} \right) + G_{12} \left(A_{22}G_{12} - B_{12}B_{22} \right) \right\}$$

$$b_6 = B_{12}G_{22} - B_{22}G_{12}$$

$$b_7 = -B_{12}B_{22} + G_{12}A_{22}$$

with

$$b_c = \left(A_{22}G_{22} - B_{22}^2 \right)^{-1}$$

and k_1 and k_2 are tracing constants (shear coefficients).

The matrix $\left[I_1 \right]$ is a 5×5 diagonal submatrix given by:

$$\left[I_1 \right] = \begin{bmatrix} -1 & & & & \\ & -1 & & & \\ & & 1 & & \\ & & & 1 & \\ & & & & 1 \end{bmatrix}$$

The nonzero terms in the symmetric mass matrices $\left[m^a \right]$ and $\left[m^b \right]$ are given by:

$$m_{33}^a = k\, m_0$$

$$m_{35}^a = k_r\, k\, m_1$$

$$m_{44}^{a} = k \, m_0$$

$$m_{55}^{a} = k_r \, k \, m_2$$

and

$$m_{11}^{b} = k \, m_0$$

$$m_{12}^{b} = k_r \, k \, m_1$$

$$m_{22}^{b} = k_r \, k \, m_2$$

where

$$k = \rho \frac{L^2}{\tilde{C}_0}$$

k_r is a tracing constant and

$$\lfloor m_0 \quad m_1 \quad m_2 \rfloor = \sum_{k=1}^{NL} \int_{h_{k-1}}^{h_k} \rho_s^{(k)} \left\lfloor 1 \quad \frac{x_3}{L} \quad \frac{x_3^2}{L^2} \right\rfloor dx_3$$

with $\rho_s^{(k)}$ being the mass density of the kth layer of the shell.

The components of the load vectors are given by:

$$\{P_{1,m}\}^T = \rho \frac{L}{\tilde{C}_0} \begin{bmatrix} \cdot & \cdot & p_{\theta,m} & p_{r,m} & \cdot \end{bmatrix}$$

$$\{P_{2,m}\}^T = \rho \frac{L}{\tilde{C}_0} \begin{bmatrix} p_{\xi,m} & \cdot & \cdot & \cdot & \cdot \end{bmatrix}$$

REFERENCES

1. Anderson, M. S.; Fulton, R. E.; Heard, W. L., Jr.; and Walz, J. E.: Stress, Buckling, and Vibration Analysis of Shells of Revolution. Computers & Structures, vol. 1, nos. 1/2, Aug. 1971, pp. 157-192.

2. Forsberg, K.; and Hartung, R.: An Evaluation of Finite Difference and Finite Element Techniques for Analysis of General Shells. High Speed Computing of Elastic Structures, Tome II, Univ. de Liège, 1971, pp. 837-859.

3. Greenbaum, Gilbert A.; and Cappelli, Anthony P.: The Numerical Methods of Discrete Shell Analysis. Computer Oriented Analysis of Shell Structures, Richard F. Hartung, ed., AFFDL-TR-71-79, U.S. Air Force, June 1971, pp. 34-64.

4. Bushnell, David: Analysis of Buckling and Vibration of Ring-Stiffened, Segmented Shells of Revolution. Int. J. Solid Structures, vol. 6, no. 1, Jan. 1970, pp. 157-181.

5. Budiansky, Bernard; and Radkowski, Peter P.: Numerical Analysis of Unsymmetrical Bending of Shells of Revolution. AIAA J., vol. 1, no. 8, Aug. 1963, pp. 1833-1842.

6. Tene, Yair: Deformation of Asymmetrically Loaded, Symmetrically Prestressed Orthotropic Shells of Revolution. AIAA J., vol. 6, no. 8, Aug. 1968, pp. 1599-1602.

7. Goldberg, John E.: Computer Analysis of Shells. Proceedings – Symposium on the Theory of Shells To Honor Lloyd Hamilton Donnell, D. Muster, ed., Univ. of Houston, 1967, pp. 3-22.

8. Kalnins, Arturs: Static, Free Vibration, and Stability Analysis of Thin, Elastic Shells of Revolution. AFFDL-TR-68-144, U.S. Air Force, Mar. 1969.

9. Cohen, Gerald A.: User Document for Computer Programs for Ring-Stiffened Shells of Revolution. NASA CR-2086, 1973.

10. Wunderlich, W.: Zur Berechnung von Rotationsschalen mit Übertragungsmatrizen. Ing. Arch., Bd. XXXVI, Heft 4, 1967, pp. 262-279.

11. Jenkins, Ronald S.; and Tottenham, Hugh: The Solution of Shell Problems by the Matrix Progression Method. Proceedings of the World Conference on Shell Structures, Nat. Acad. Sci., c.1964, pp. 563-579.

12. Greenbaum, G. A.; and Conroy, D. C.: Postwrinkling Behavior of a Conical Shell of Revolution Subjected to Bending Loads. AIAA J., vol. 8, no. 4, Apr. 1970, pp. 700-707.

13. Stephens, Wendell B.; and Fulton, Robert E.: Axisymmetric Static and Dynamic Buckling of Spherical Caps Due to Centrally Distributed Pressures. AIAA J., vol. 7, no. 11, Nov. 1969, pp. 2120-2126.

14. Forsberg, Kevin: A Review of Analytical Methods Used To Determine the Modal Characteristics of Cylindrical Shells. NASA CR-613, 1966.

15. Heard, Walter L., Jr.; Anderson, Melvin S.; and Chen, Ming M.: Computer Program for Structural Analysis of Layered Orthotropic Ring-Stiffened Shells of Revolution (SALORS) — Linear Stress Analysis Option. NASA TN D-7179, 1973.

16. Stein, Manuel: The Influence of Prebuckling Deformations and Stresses on the Buckling of Perfect Cylinders. NASA TR R-190, 1964.

17. Noor, A. K.; and Khandelwal, V. K.: Improved Finite-Difference Variant for the Bending Analysis of Arbitrary Cylindrical Shells. UNICIV Rep. No. R-58, Univ. of New South Wales, Dec. 1969.

18. Sylvester, R. J.; and Meyer, F.: Two Point Boundary Problems by Quasilinearization. J. Soc. Ind. Appl. Math., vol. 13, no. 2, June 1965, pp. 586-602.

19. Fox, L.: The Numerical Solution of Two-Point Boundary Problems in Ordinary Differential Equations. Clarendon Press (Oxford), 1957.

TABLE 1.- CHARACTERISTICS OF FINITE-DIFFERENCE SCHEMES

USED IN THE PRESENT STUDY

	Finite-difference scheme					
	DW	SW	MW	MHS 1	MHS 2	MHI
Shell theory used	Flügge-Lure-Byrne theory	Sanders–Budiansky first approximation theory				
Shear deformation and rotary inertia	Neglected				Accounted for	
Fundamental unknowns	U_ξ, U_θ, W	U_ξ, U_θ, W, M_ξ	N_ξ, M_ξ, U_ξ, U_θ, W, ϕ_θ, U_ξ, ϕ_ξ, $\check{N}_{\xi\theta}$, Q_ξ, $\check{M}_{\xi\theta}$			
Governing differential equations	Two second-order equations and one fourth-order equation	Four second-order equations	Ten first-order equations			
Difference-quotient expression used for first derivatives	$\partial F\vert_i \approx \frac{1}{2\ell}(-F_{i-2} + F_{i+2})$			$\frac{1}{2}(\partial F\vert_i + \partial F\vert_{i+2}) \approx \frac{1}{\ell}(-F_i + F_{i+2})$		$\partial F\vert_{i+1} \approx \frac{1}{\ell}(-F_i + F_{i+2})$
Points at which eqs. (17) are applied	Node points i, i±2, i±4, ...			Points lying midway between node points (i±1, i±3, ...)		Eqs. (17a) at node points, and eqs. (17b) at points lying midway between node points.
	Ref. 14	Refs. 1, 5, & 15	Ref. 19	Refs. 19 and 12	Refs. 13 and 18	
Bandwidth of resulting finite-difference field equations [a]	17	15	31 b(25)	29 b(23)	29 b(23)	19 b(15)

a The boundary discretization errors in schemes SW, DW, MW, and MHI are assumed to be of order $O(\ell)$.

b Corresponding bandwidth if classical theory (with shear deformation neglected) is used and hence the governing differential equations reduce to eight first-order equations.

TABLE 2.- CONVERGENCE OF MINIMUM NONDIMENSIONAL FREQUENCY λ OBTAINED BY DIFFERENT FINITE-DIFFERENCE SCHEMES

$$\left[\text{Clamped isotropic cylindrical shell with } h/R = 0.002,\right.$$
$$\left. L/R = 10, \quad \nu = 0.3, \text{ and } m = 4; \quad \lambda = 100\,\omega R\,\sqrt{\rho_S(1 - \nu^2)/E}\right]$$

n	Values of λ for –			
	SW and DW	MW	MHS 1 and MHS 2	MHI
10	2.101 [a](1.393)	1.398 (0.665)	1.549 (1.027)	1.485 (0.985)
20	1.689 (1.120)	1.485 (0.985)	1.517 (1.006)	1.506 (0.999)
30	1.593 (1.056)	1.501 (0.995)	1.512 (1.003)	1.508 (1.000)

[a]Numbers in parentheses refer to $\omega/\omega_{\text{converged}}$.

TABLE 3.- ERROR INDEX FOR STRESS RESULTANTS AND GENERALIZED DISPLACEMENTS OBTAINED BY DIFFERENT FINITE-DIFFERENCE SCHEMES

$$\left[\text{Closed toroidal shell problem,} \quad E_f = \frac{1}{n+1} \sqrt{\sum_{i=1}^{n+1} \left(\frac{f_i - \widehat{f}_i}{f_{max}} \right)^2} \right]$$

n	Values of $E_f \times 100$ for —			
	MW	MHS 1	MHS 2	MHI
$f = N_\xi$				
10	6.935	1.043	1.275	1.121
20	.339	.186	.250	.179
30	.132	.068	.093	.065
40	.065	.033	.046	.031
$f = M_\xi$				
10	26.369	6.683	5.248	2.320
20	3.990	1.420	1.056	.459
30	1.232	.536	.392	.167
40	.571	.265	.193	.081
$f = M_{\xi\theta}$				
10	35.352	6.956	5.813	2.369
20	4.602	1.620	1.288	.515
30	1.426	.652	.531	.250
40	.675	.359	.308	.184
$f = U_\theta$				
10	47.157	8.385	7.760	1.524
20	5.301	1.838	1.663	.294
30	1.610	.692	.623	.107
40	.742	.341	.307	.052
$f = W$				
10	42.524	7.737	6.769	2.096
20	5.112	1.744	1.444	.355
30	1.550	.664	.543	.129
40	.716	.329	.268	.062
$f = U_\xi$				
10	37.404	6.221	5.590	1.390
20	4.256	1.470	1.277	.270
30	1.320	.581	.503	.115
40	.622	.307	.269	.096
$f = \phi_\theta$				
10	43.012	7.804	6.896	1.326
20	4.939	1.703	1.426	.231
30	1.492	.641	.531	.084
40	.687	.316	.261	.040
$f = \phi_\xi$				
10	30.989	6.778	5.355	2.806
20	4.548	1.621	1.221	.549
30	1.384	.667	.520	.223
40	.648	.376	.311	.162

TABLE 4.- CONVERGENCE OF MINIMUM NONDIMENSIONAL FREQUENCY

OBTAINED BY DIFFERENT FINITE-DIFFERENCE SCHEMES

$$\left[\text{Clamped graphite-epoxy spherical shell with } h/R = 0.002; \ m = 2; \ \lambda_1 = \omega \sqrt{\rho h^2 / E_T}\right]$$

n	Values of $\lambda_1 \times 10^3$ for –				Converged solution
	MW	MHS 1	MHS 2	MHI	
$\theta = \dfrac{\pi}{2}$ (hemispherical shell)					
10	2.7962	2.7830	2.8614	2.8403	2.8217
20	2.8099	2.7909	2.8302	2.8257	
30	2.8146	2.8095	2.8266	2.8239	
40	2.8166	2.8136	2.8246	2.8231	
$\theta = \dfrac{\pi}{6}$					
10	3.4550	3.6456	3.7724	3.6489	3.6644
20	3.6140	3.6789	3.6882	3.6614	
30	3.6411	3.6704	3.6760	3.6634	
40	3.6508	3.6666	3.6713	3.6640	
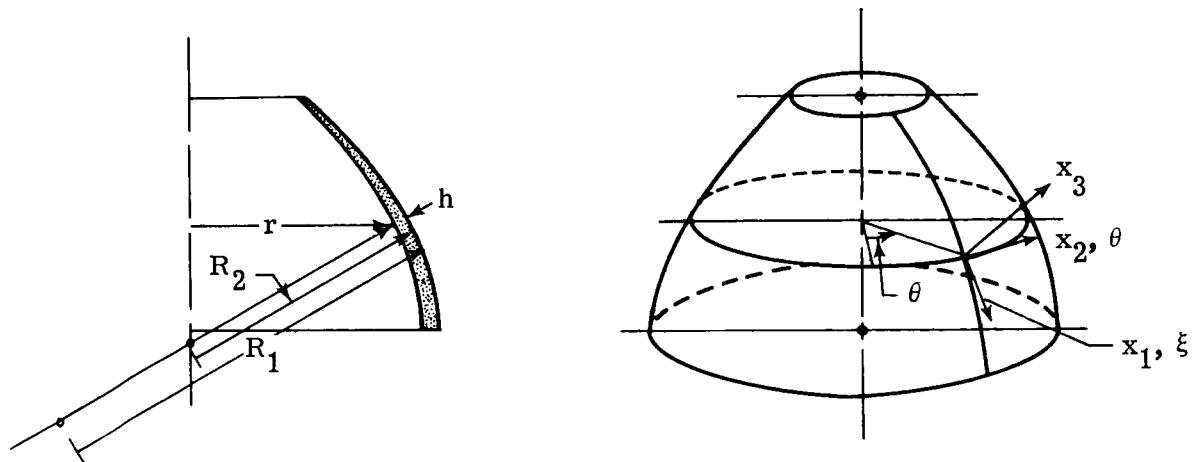
Figure 1.- Shell geometry.
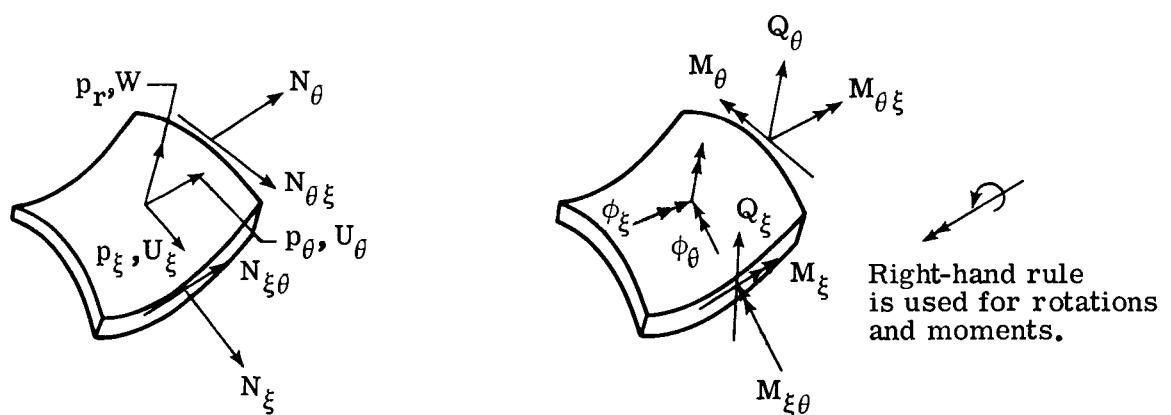
Figure 2.- Sign convention for stress resultants and displacements.
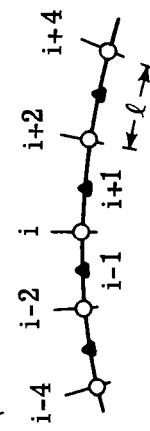
(a) Interior points.
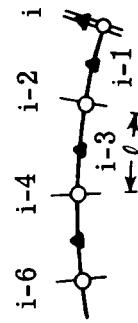
(b) Boundary points.
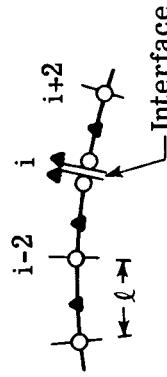
(c) Discontinuity or interface.

Designation	Location	Equation applied	Functions defined at the points
O	Interior, boundary and interface	Eqs. (17a)	$\{H_m\}$ and $\{d\psi_m\}$
	Interior	Eqs. (17b)	$\{\psi_m\}$ and $\{dH_m\}$
▲	Boundary	Boundary conditions	$\{\psi_m\}$
	Interface	Interface conditions	

Figure 3.- Control points for the different fundamental unknowns in the MHI scheme.

| Point	$\{H_m\}_1$	$\{\psi_m\}_1$	$\{H_m\}_3$	$\{\psi_m\}_3$	$\{H_m\}_5$	$\{\psi_m\}_5$	$\{H_m\}_7$	$\{\psi_m\}_7$	$\{H_m\}_9$	$\{\psi_m\}_9$	External force vectors
1		Boundary conditions									Boundary effects
1	$[S^a]_1$	$[S]_1$ $-\frac{1}{\ell}[I_1]$		$\frac{1}{\ell}[I_1]$							$\{P_{1,m}\}_1$
3		$\frac{-1}{2\ell}[I_1]$	$[S^a]_3$	$[S]_3$		$\frac{1}{2\ell}[I_1]$					$\{P_{1,m}\}_3$
3	$\frac{1}{2\ell}[I_1]$		$[S]_3^T$	$[S^b]_3$	$\frac{-1}{2\ell}[I_1]$						$\{P_{2,m}\}_3$
5				$\frac{-1}{2\ell}[I_1]$	$[S^a]_5$	$[S]_5$		$\frac{1}{2\ell}[I_1]$			$\{P_{1,m}\}_5$
5			$\frac{1}{2\ell}[I_1]$		$[S]_5^T$	$[S^b]_5$	$\frac{-1}{2\ell}[I_1]$				$\{P_{2,m}\}_5$
7						$\frac{-1}{2\ell}[I_1]$	$[S^a]_7$	$[S]_7$		$\frac{1}{2\ell}[I_1]$	$\{P_{1,m}\}_7$
7					$\frac{1}{2\ell}[I_1]$		$[S]_7^T$	$[S^b]_7$	$\frac{-1}{2\ell}[I_1]$		$\{P_{2,m}\}_7$
9								$\frac{-1}{\ell}[I_1]$	$[S^a]_9$	$[S]_9$ $+\frac{1}{\ell}[I_1]$	$\{P_{1,m}\}_9$
9									Boundary conditions		Boundary effects

(a) MW scheme.

Figure 4.- Schematic representation of the finite-difference equations obtained by the first-order equation schemes.

| Point	$\{\psi_m\}_1$	$\{H_m\}_1$	$\{\psi_m\}_2$	$\{H_m\}_3$	$\{\psi_m\}_4$	$\{H_m\}_5$	$\{\psi_m\}_6$	$\{H_m\}_7$	$\{\psi_m\}_8$	$\{H_m\}_9$	$\{\psi_m\}_9$	External force vectors
	Boundary conditions											Boundary effects
1	$[s]_1$ $\frac{-2}{\ell}[I_1]$	$[s^a]_1$	$\frac{2}{\ell}[I_1]$									$\{P_{1,m}\}_1$
2		$\frac{1}{2}[s]_2^T + \frac{1}{\ell}[I_1]$	$[s^b]_2$	$\frac{1}{2}[s]_2^T - \frac{1}{\ell}[I_1]$								$\{P_{2,m}\}_2$
3			$\frac{1}{2}[s]_3 - \frac{1}{\ell}[I_1]$	$[s^a]_3$	$\frac{1}{2}[s]_3 + \frac{1}{\ell}[I_1]$							$\{P_{1,m}\}_3$
4				$\frac{1}{2}[s]_4^T + \frac{1}{\ell}[I_1]$	$[s^b]_4$	$\frac{1}{2}[s]_4^T - \frac{1}{\ell}[I_1]$						$\{P_{2,m}\}_4$
5					$\frac{1}{2}[s]_5 - \frac{1}{\ell}[I_1]$	$[s^a]_5$	$\frac{1}{2}[s]_5 + \frac{1}{\ell}[I_1]$					$\{P_{1,m}\}_5$
6						$\frac{1}{2}[s]_6^T + \frac{1}{\ell}[I_1]$	$[s^b]_6$	$\frac{1}{2}[s]_6^T - \frac{1}{\ell}[I_1]$				$\{P_{2,m}\}_6$
7							$\frac{1}{2}[s]_7 - \frac{1}{\ell}[I_1]$	$[s^a]_7$	$\frac{1}{2}[s]_7 + \frac{1}{\ell}[I_1]$			$\{P_{1,m}\}_7$
8								$\frac{1}{2}[s]_8^T - \frac{1}{\ell}[I_1]$	$[s^b]_8$	$\frac{1}{2}[s]_8^T + \frac{1}{\ell}[I_1]$		$\{P_{2,m}\}_8$
9									$\frac{-2}{\ell}[I_1]$	$[s^a]_9$	$[s]_9 + \frac{2}{\ell}[I_1]$	$\{P_{1,m}\}_9$
									Boundary conditions			Boundary effects

(b) MHI scheme.

Figure 4.- Continued.

Point	$\{H_m\}_1$	$\{\psi_m\}_1$	$\{H_m\}_3$	$\{\psi_m\}_3$	$\{H_m\}_5$	$\{\psi_m\}_5$	$\{H_m\}_7$	$\{\psi_m\}_7$	$\{H_m\}_9$	$\{\psi_m\}_9$	External force vectors
1	Boundary conditions										Boundary effects
2	$\frac{1}{2}[S^a]_1$	$\frac{1}{2}[S]_1 - \frac{1}{\ell}[I_1]$	$\frac{1}{2}[S^a]_3$	$\frac{1}{2}[S]_3 + \frac{1}{\ell}[I_1]$							$\frac{1}{2}\{P_{1,m}\}_1 + \frac{1}{2}\{P_{1,m}\}_3$
	$\frac{1}{2}[S]_1^T + \frac{1}{\ell}[I_1]$	$\frac{1}{2}[S^b]_1$	$\frac{1}{2}[S]_3^T - \frac{1}{\ell}[I_1]$	$\frac{1}{2}[S^b]_3$							$\frac{1}{2}\{P_{2,m}\}_1 + \frac{1}{2}\{P_{2,m}\}_3$
4			$\frac{1}{2}[S^a]_3$	$\frac{1}{2}[S]_3 - \frac{1}{\ell}[I_1]$	$\frac{1}{2}[S^a]_5$	$\frac{1}{2}[S]_5 + \frac{1}{\ell}[I_1]$					$\frac{1}{2}\{P_{1,m}\}_3 + \frac{1}{2}\{P_{1,m}\}_5$
			$\frac{1}{2}[S]_3^T + \frac{1}{\ell}[I_1]$	$\frac{1}{2}[S^b]_3$	$\frac{1}{2}[S]_5^T - \frac{1}{\ell}[I_1]$	$\frac{1}{2}[S^b]_5$					$\frac{1}{2}\{P_{2,m}\}_3 + \frac{1}{2}\{P_{2,m}\}_5$
6					$\frac{1}{2}[S^a]_5$	$\frac{1}{2}[S]_5 - \frac{1}{\ell}[I_1]$	$\frac{1}{2}[S^a]_7$	$\frac{1}{2}[S]_7 + \frac{1}{\ell}[I_1]$			$\frac{1}{2}\{P_{1,m}\}_5 + \frac{1}{2}\{P_{1,m}\}_7$
					$\frac{1}{2}[S]_5^T + \frac{1}{\ell}[I_1]$	$\frac{1}{2}[S^b]_5$	$\frac{1}{2}[S]_7^T - \frac{1}{\ell}[I_1]$	$\frac{1}{2}[S^b]_7$			$\frac{1}{2}\{P_{2,m}\}_5 + \frac{1}{2}\{P_{2,m}\}_7$
8							$\frac{1}{2}[S^a]_7$	$\frac{1}{2}[S]_7 - \frac{1}{\ell}[I_1]$	$\frac{1}{2}[S^a]_9$	$\frac{1}{2}[S]_9 + \frac{1}{\ell}[I_1]$	$\frac{1}{2}\{P_{1,m}\}_7 + \frac{1}{2}\{P_{1,m}\}_9$
							$\frac{1}{2}[S]_7^T + \frac{1}{\ell}[I_1]$	$\frac{1}{2}[S^b]_7$	$\frac{1}{2}[S]_9^T - \frac{1}{\ell}[I_1]$	$\frac{1}{2}[S^b]_9$	$\frac{1}{2}\{P_{2,m}\}_7 + \frac{1}{2}\{P_{2,m}\}_9$
9									Boundary conditions		Boundary effects

(c) MHS 1 scheme.

Figure 4.- Continued.
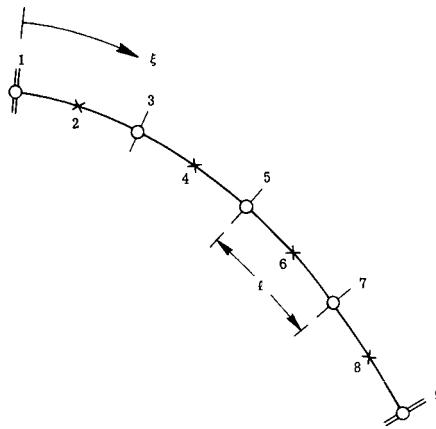
Points	$\{H_m\}_1$	$\{\psi_m\}_1$	$\{H_m\}_3$	$\{\psi_m\}_3$	$\{H_m\}_5$	$\{\psi_m\}_5$	$\{H_m\}_7$	$\{\psi_m\}_7$	$\{H_m\}_9$	$\{\psi_m\}_9$	External force vectors
1	Boundary conditions										Boundary effects
2	$\frac{1}{2}[S^a]_2$	$\frac{1}{2}[S]_2 - \frac{1}{\ell}[I_1]$	$\frac{1}{2}[S^a]_2$	$\frac{1}{2}[S]_2 + \frac{1}{\ell}[I_1]$							$\{P_{1,m}\}_2$
	$\frac{1}{2}[S]_2^T + \frac{1}{\ell}[I_1]$	$\frac{1}{2}[S^b]_2$	$\frac{1}{2}[S]_2^T - \frac{1}{\ell}[I_1]$	$\frac{1}{2}[S^b]_2$							$\{P_{2,m}\}_2$
4			$\frac{1}{2}[S^a]_4$	$\frac{1}{2}[S]_4 - \frac{1}{\ell}[I_1]$	$\frac{1}{2}[S^a]_4$	$\frac{1}{2}[S]_4 + \frac{1}{\ell}[I_1]$					$\{P_{1,m}\}_4$
			$\frac{1}{2}[S]_4^T + \frac{1}{\ell}[I_1]$	$\frac{1}{2}[S^b]_4$	$\frac{1}{2}[S]_4^T - \frac{1}{\ell}[I_1]$	$\frac{1}{2}[S^b]_4$					$\{P_{2,m}\}_4$
6					$\frac{1}{2}[S^a]_6$	$\frac{1}{2}[S]_6 - \frac{1}{\ell}[I_1]$	$\frac{1}{2}[S^a]_6$	$\frac{1}{2}[S]_6 + \frac{1}{\ell}[I_1]$			$\{P_{1,m}\}_6$
					$\frac{1}{2}[S]_6^T + \frac{1}{\ell}[I_1]$	$\frac{1}{2}[S^b]_6$	$\frac{1}{2}[S]_6^T - \frac{1}{\ell}[I_1]$	$\frac{1}{2}[S^b]_6$			$\{P_{2,m}\}_6$
8							$\frac{1}{2}[S^a]_8$	$\frac{1}{2}[S]_8 - \frac{1}{\ell}[I_1]$	$\frac{1}{2}[S^a]_8$	$\frac{1}{2}[S]_8 + \frac{1}{\ell}[I_1]$	$\{P_{1,m}\}_8$
							$\frac{1}{2}[S]_8^T + \frac{1}{\ell}[I_1]$	$\frac{1}{2}[S^b]_8$	$\frac{1}{2}[S]_8^T - \frac{1}{\ell}[I_1]$	$\frac{1}{2}[S^b]_8$	$\{P_{2,m}\}_8$
9									Boundary conditions		Boundary effects

(d) MHS 2 scheme.

Figure 4.- Concluded.
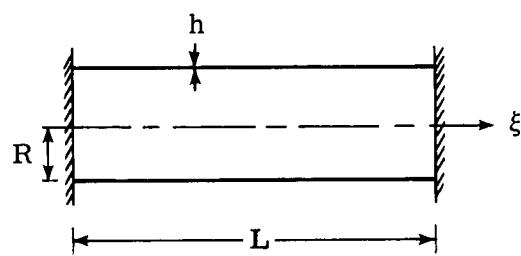
h/R $\approx$ 0.002
L/R $\approx$ 10
$\nu \approx 0.3$

Figure 5.- Characteristics of isotropic cylindrical
shell used in the present study.
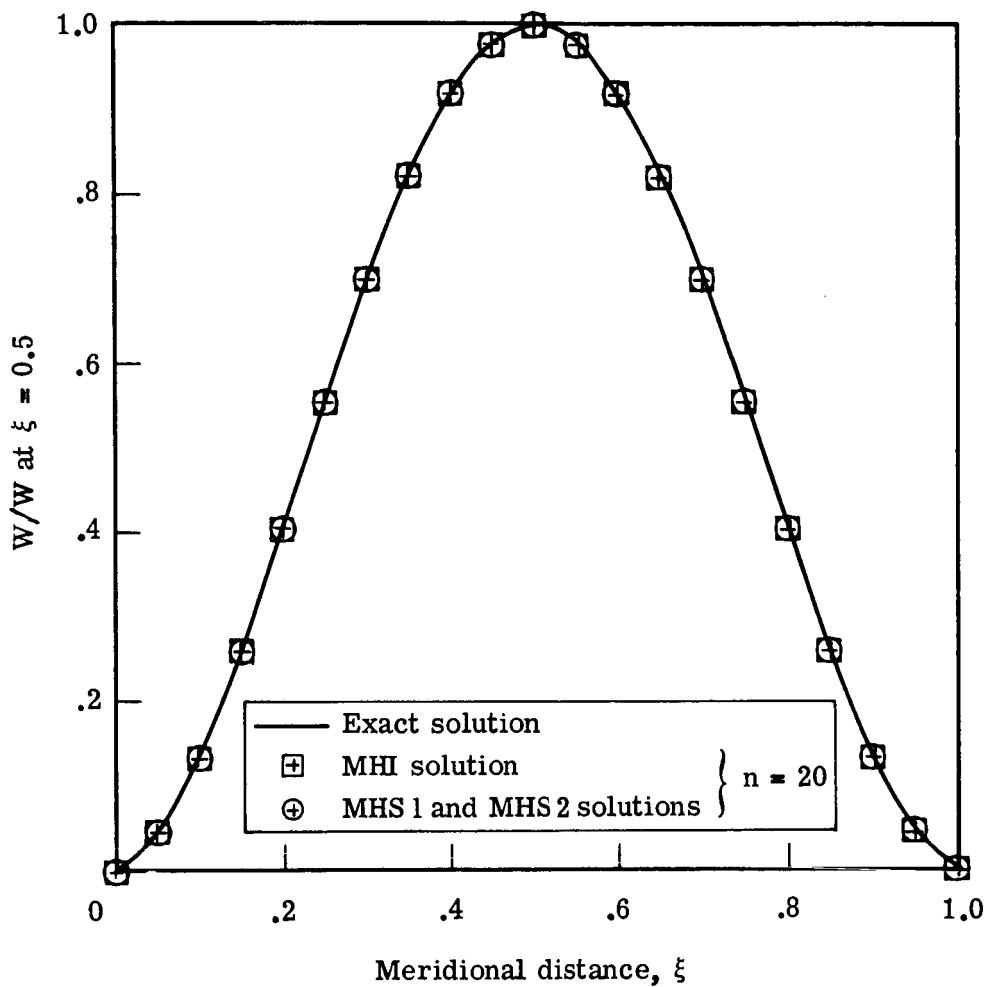
(a) Normal displacement, W.

Figure 6.- Mode shapes and modal stress resultants obtained by MHS 1, MHS 2, and MHI schemes for isotropic circular cylindrical shell.
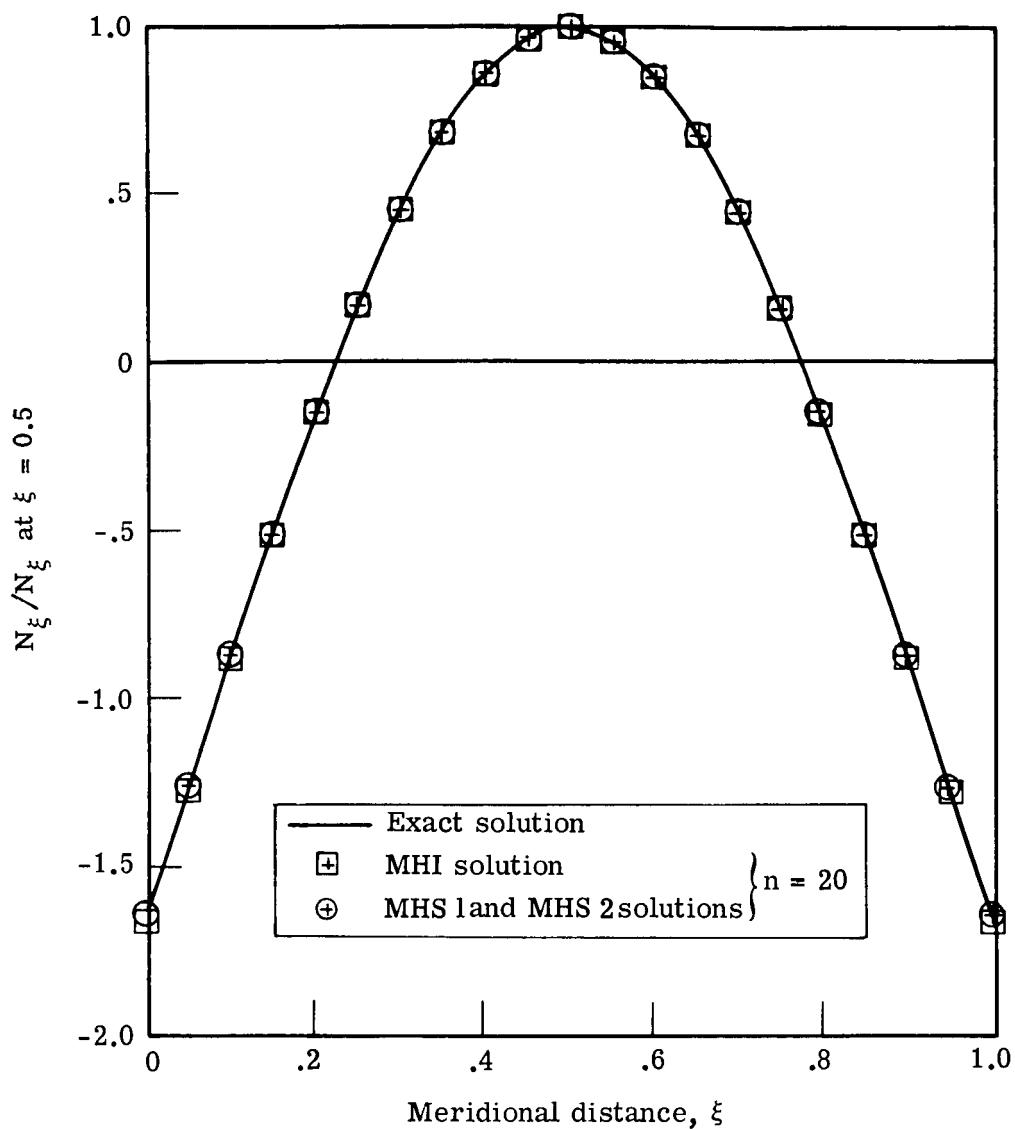
(b) Meridional stress resultant, N_ξ.

Figure 6.- Continued.

Legend:
—— Exact solution M_ξ/M_ξ at $\xi = 0$
⊞ MHI solution $-M_\xi/2M_\xi$ at $\xi = 0.5$
⊕ MHS 1 and MHS 2 solutions M_ξ/M_ξ at $\xi = 0$ $\Big\} n = 20$

(c) Meridional moment stress resultant, M_ξ.

Figure 6.- Concluded.

h/R = 0.02
a/R = 0.50
ν = 0.30

Fourier harmonic in circumferential
direction, m = 2

$$p_r = p_o \cos m\theta$$
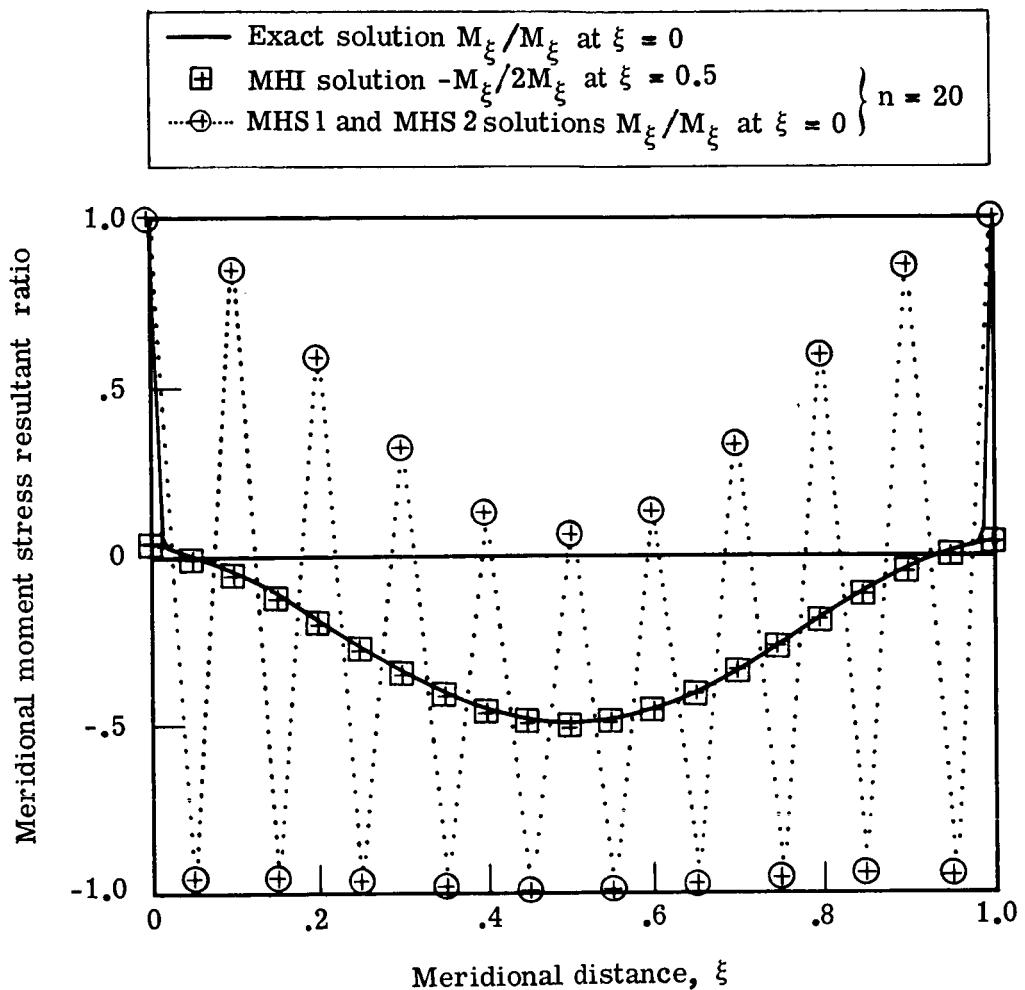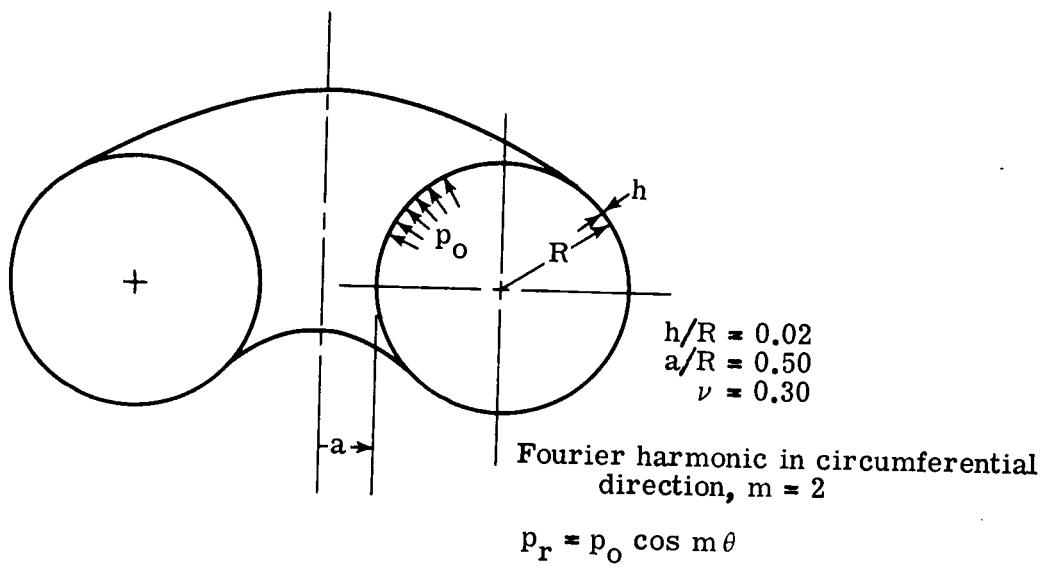
Figure 7.- Characteristics of toroidal shell and loading.
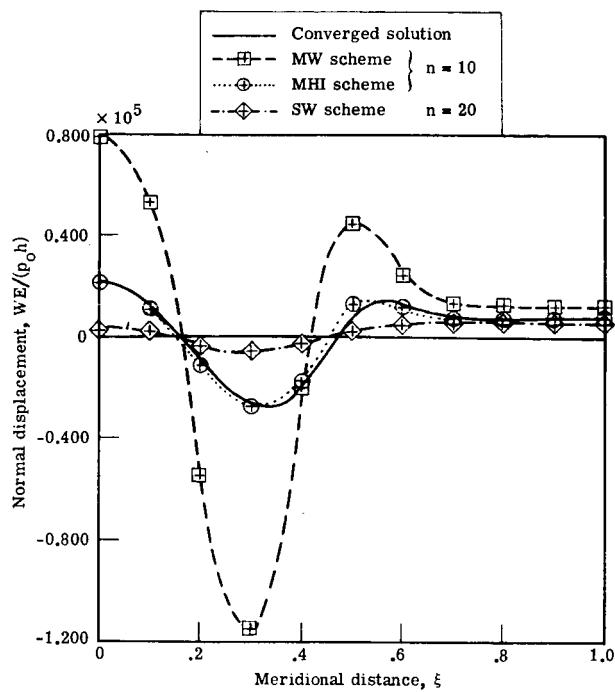
(a) Normal displacement.
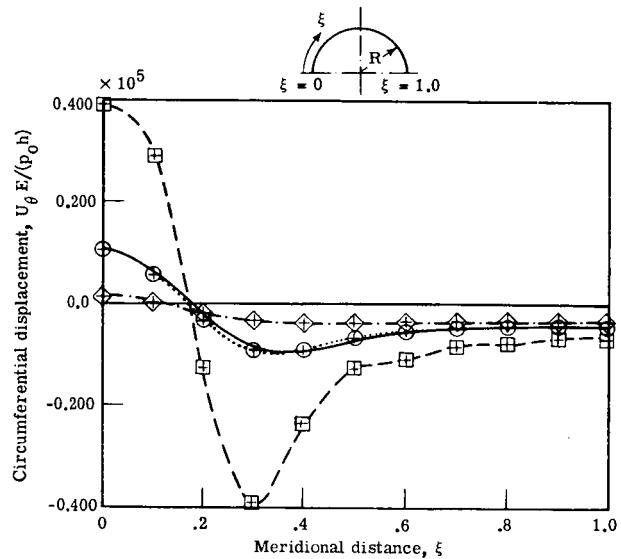
(b) Circumferential displacement.
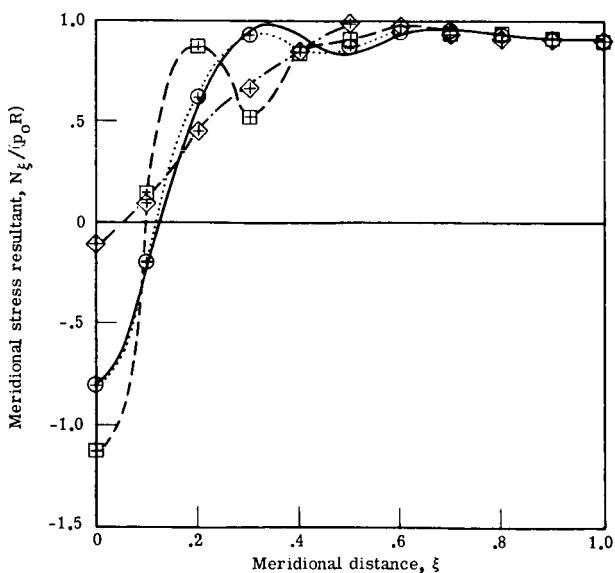
(c) Meridional stress resultant.
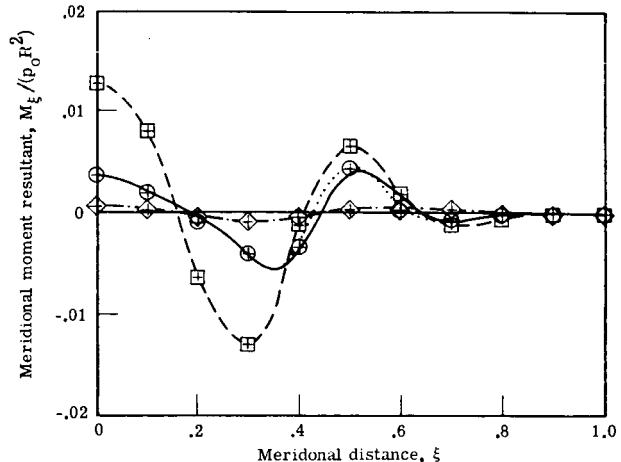
(d) Meridional moment stress resultant.

Figure 8.- Accuracy of stress resultants and displacements obtained by different finite-difference schemes for a toroidal shell with a uniform internal pressure p_r; $m = 2$.
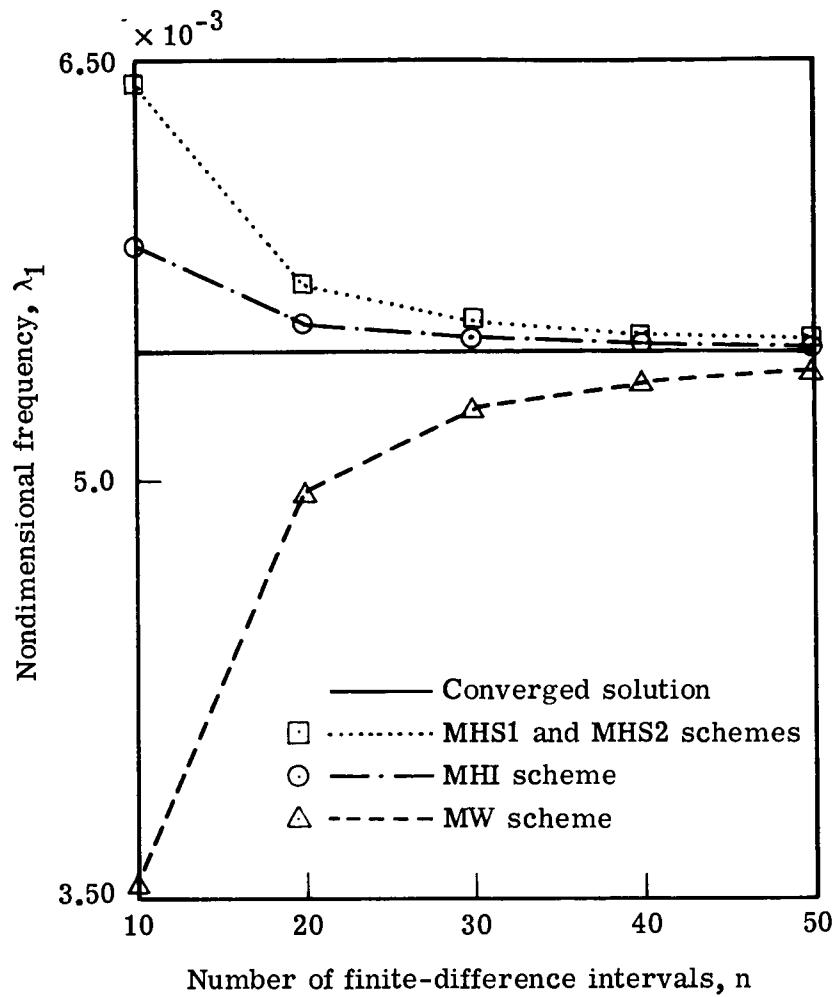
Figure 9.- Convergence of minimum frequency obtained by different finite-difference schemes based on the first-order equation formulation (graphite-epoxy toroidal shell with $h/R = 0.02$; $m = 2$).

Fibers of top layer in the meridional direction

Middle surface

$E_L/E_T = 30$
$G_{LT}/E_T = 0.60$
$G_{TT}/E_T = 0.50$
$\nu_{LT} = 0.25$
$h/R = 0.002$
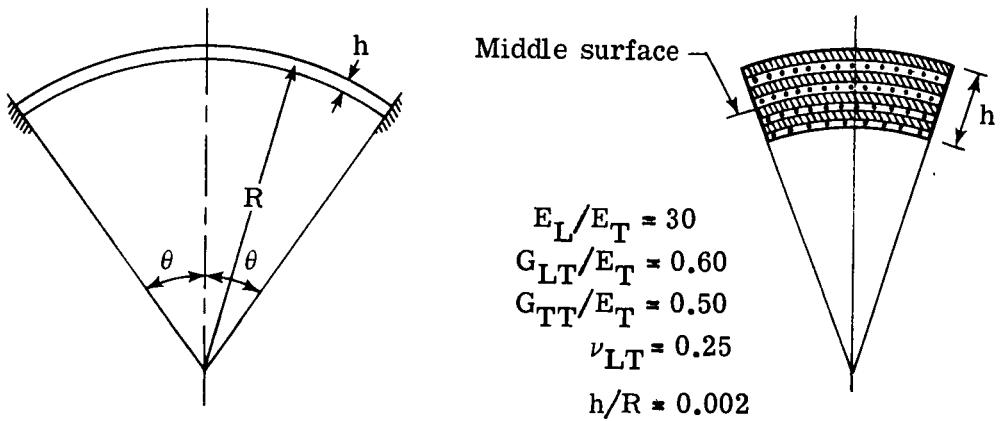
Subscripts L and T refer to direction of
fibers and transverse direction,
respectively.

Figure 10.- Eight-layered graphite-epoxy spherical shell with clamped edges.